



On the quintic time-dependent coefficient derivative nonlinear Schrödinger equation in hydrodynamics or fiber optics

Ting-Ting Jia · Yi-Tian Gao · Yu-Jie Feng · Lei Hu · Jing-Jing Su · Liu-Qing Li · Cui-Cui Ding

Received: 1 November 2018 / Accepted: 14 January 2019 / Published online: 14 February 2019
© Springer Nature B.V. 2019

Abstract Under investigation in this paper is a quintic time-dependent coefficient derivative nonlinear Schrödinger equation for certain hydrodynamic wave packets or a medium with the negative refractive index. A gauge transformation is found to obtain the equivalent form of the equation. With respect to the wave envelope for the free water surface displacement or envelope of the electric field, Painlevé integrable condition, different from that in the existing literature, is derived, with which the bilinear forms and N -soliton solutions are constructed. Asymptotic analysis illustrates that the interactions between the bright and bound solitons as well as between the bright solitons and Kuznetsov–Ma breathers are elastic with certain conditions, while some other interactions are inelastic under other conditions. Propagation paths and velocities for the solitons are both affected by the dispersion coefficient function when the relations among the coefficients are linear, or affected by the dispersion coefficient, self-steepening coefficient and cubic nonlinearity functions when the relations among the coefficients are nonlinear. Under different conditions, bell-shaped solitons can evolve into the bound solitons or Kuznetsov–Ma breathers, respectively. Interactions between the bright

and parabolic (or hyperbolic) solitons are related to the dispersion coefficient, self-steepening coefficient and cubic nonlinearity functions. Compression effect on the propagation paths of the solitons, caused by the dispersion coefficient, is observed.

Keywords Quintic time-dependent coefficient derivative nonlinear Schrödinger equation · Equivalent form · Painlevé analysis · Bilinear forms · N -soliton solutions · Breathers

1 Introduction

In recent years, there have been a variety of researches on the nonlinear evolution equations (NLEEs) [1–27]. Studies on the interactions of the localized waves have been extended to the higher-order and higher-dimensional NLEEs [8–27] and multi-component coupled NLEEs [28–37].

Derivative nonlinear Schrödinger (DNLS) equations have been investigated due to the applications in plasmas, fluids and fiber optics [38–45]. Quintic DNLS equations have been applied in the media with negative refractive indices, inhomogeneous plasmas and hydrodynamic wave packets [46–51]. A quintic time-dependent coefficient DNLS equation,

$$iu_t + \lambda(t) u_{xx} + i\alpha(t) |u|^2 u_x + \mu(t) |u|^2 u + \nu(t) |u|^4 u = 0, \quad (1)$$

T.-T. Jia · Y.-T. Gao (✉) · Y.-J. Feng · L. Hu · J.-J. Su · L.-Q. Li · C.-C. Ding
Ministry-of-Education Key Laboratory of Fluid Mechanics and National Laboratory for Computational Fluid Dynamics, Beijing University of Aeronautics and Astronautics, Beijing 100191, China
e-mail: gaoyt163@163.com

has been used to describe certain hydrodynamic wave packets [48] or a medium with the negative refractive index [51], where $i = \sqrt{-1}$, $u(x, t)$ is the wave envelope for the free water surface displacement or envelope of the electric field [50], $\mu(t)$ and $\nu(t)$ represent the cubic and quintic nonlinearities, respectively, $\lambda(t)$ denotes the dispersion coefficient, $\alpha(t)$ is the self-steepening coefficient, t and x denote not only the slow time and spatial coordinate traveling with the group velocity in hydrodynamics, but also the propagation distance and retarded time in the context of optical fiber physics [48, 51]. A class of the chirped soliton-like solutions including the bright and kink solitons for Eq. (1) has been derived via the trial equation method [51]. Special cases of Eq. (1) have been seen as follows:

- When $[\lambda(t), \alpha(t), \mu(t), \nu(t)] = [1, -1, 0, \frac{1}{2}]$, Eq. (1) has been reduced to the Gerdjikov–Ivanov equation in the Madelung fluid [47]. Constraints on the soliton types have been derived, including the bright soliton, dark soliton, up-shifted bright, upper-shifted bright, gray soliton and black soliton types [47].
- When $\lambda(t), \alpha(t), \mu(t)$ and $\nu(t)$ are the constant coefficients, Eq. (1) has been reduced to the quintic DNLS equation in hydrodynamics or fiber optics [48, 50], to describe how a water wave packet deforms and eventually is destroyed as it propagates shoreward from the deep to shallow water via the Newton–Raphson method [50]. “Gray” soliton on a continuous-wave background, i.e., the “dark” localized mode with a nonzero minimum in the intensity, has been derived via two integrals of motion [48].
- When $[\lambda(t), \alpha(t), \mu(t), \nu(t)] = [1, 1, 0, 0]$, Eq. (1) has been reduced to the Chen–Lee–Liu equation for the nonlinear optical pulses in a quadratic nonlinear crystal involving the self-steepening without any concomitant self-phase-modulation [43], with the soliton, breather, multi-rogue wave and rational solutions constructed [45].

Painlevé analysis has been used to derive the Painlevé integrable condition and transformation for the bilinear forms [52–55]. Asymptotic analysis has been used to investigate the solitons before and after the interactions, with which the relevant physical properties of the solitons have been derived [56, 57].

However, to our knowledge, under the constraint different from that in Ref. [48], the effects of the time-

dependent coefficients $\alpha(t)$, $\lambda(t)$, $\mu(t)$ and $\nu(t)$ on the interactions among the solitons for Eq. (1) have not been investigated. In Sect. 2, we will give the gauge transformation for an equivalent form of Eq. (1). In Sect. 3, Painlevé integrable condition for Eq. (1), different from that in Ref. [48], will be derived. In Sect. 4, we will obtain the bilinear forms and N -soliton solutions for Eq. (1). In Sect. 5, asymptotic analysis on the interactions among the solitons will be conducted. In Sect. 6, influence of $\alpha(t)$, $\lambda(t)$, $\mu(t)$ and $\nu(t)$ on the interactions will be discussed. In Sect. 7, we will give the conclusions.

2 Equivalent form of Eq. (1)

Motivated by Ref. [58], introducing the gauge transformation

$$\tilde{u} = ue^{-\frac{1}{2}i\kappa \int |u|^2 dx}, \quad (2)$$

we hereby find that the equation

$$i\tilde{u}_t + \lambda(t)\tilde{u}_{xx} + i\alpha(t)(|\tilde{u}|^2\tilde{u})_x + \mu(t)|\tilde{u}|^2\tilde{u} + \nu(t)|\tilde{u}|^4\tilde{u} = 0 \quad (3)$$

can be transformed to Eq. (1), where $\kappa = \frac{\lambda(t)}{\alpha(t)}$ is a nonzero real constant. Meanwhile, $|\tilde{u}| = |u|$ indicates that Transformation (2) amounts to an amplitude-dependent phase shift. We have found that Eq. (3) is the equivalent form of Eq. (1).¹

3 Painlevé analysis for Eq. (1)

Motivated by Refs. [53, 54], Painlevé integrability for Eq. (1) can be analyzed via the coupled system,

$$iu_t + \lambda(t)u_{xx} + \mu(t)u^2v + i\alpha(t)uvu_x + \nu(t)u^3v^2 = 0, \quad (4a)$$

$$iv_t - \lambda(t)v_{xx} - \mu(t)v^2u + i\alpha(t)vuv_x - \nu(t)v^3u^2 = 0, \quad (4b)$$

where $v = u^*$ and $*$ denotes the complex conjugate.

¹ By the way, Eq. (3) has been demonstrated to belong to the Kaup–Newell hierarchy [59], and when $\lambda(t) = \alpha(t) = 1$ and $\mu(t) = \nu(t) = 0$, Eq. (3) has been reduced to the Kaup–Newell equation describing the circular polarized nonlinear Alfvén waves in plasmas [60].

Motivated by Ref. [55], the solutions for Eq. (4) can be expanded in terms of the Laurent series, as follows:

$$u = \phi^{-a\gamma} \sum_{j=0}^{+\infty} q_j^a \phi^j, \quad v = \phi^{-b\beta} \sum_{j=0}^{+\infty} r_j^b \phi^j, \quad (5)$$

where ϕ , q_j and r_j are the analytic functions with respect to x and t , j is a nonnegative integer, a and b are both the real constants, while γ and β are both the positive integers.

The leading orders of the solutions for Eq. (4) are assumed as

$$u \sim q_0^a \phi^{-a\gamma}, \quad v \sim r_0^b \phi^{-b\beta}, \quad (6)$$

where r_0 and q_0 are nonzero in the neighborhood of a non-characteristic movable singularity manifold. Substituting Expressions (6) into Eq. (4) and balancing the highest-order nonlinear and linear terms, we obtain

$$a\gamma + b\beta = 1, \quad (7a)$$

$$q_0^a r_0^b = 2i(1 - 2a\gamma) \frac{\lambda(t)}{\alpha(t)} \phi_x, \quad (7b)$$

and derive the variable-coefficient constraint as

$$\alpha(t)^2 + \frac{4(2a\gamma - 1)^2}{3a\gamma(a\gamma - 1)} \lambda(t) v(t) = 0. \quad (8)$$

Then, to find the resonances, substituting

$$u \sim q_0^a \phi^{-a\gamma} + q_j^a \phi^{-a\gamma+j}, \quad v \sim r_0^b \phi^{-b\beta} + r_j^b \phi^{-b\beta+j} \quad (9)$$

into Eq. (4), we make the sum of the terms with the lowest power of ϕ in Eqs. (4a) and (4b) to vanish, respectively. Due to the arbitrariness of the corresponding q_j and r_j for the resonance point j , we can obtain

$$(j - 3)(j - 2)j(j + 1) \frac{16(2a\gamma - 1)^4}{9a^2\gamma^2(a\gamma - 1)^2} v(t)^2 \lambda(t)^2 = 0. \quad (10)$$

Due to Eq. (10), the resonances occur at $j = -1, 0, 2$ and 3 , while $j = -1$ corresponds to the arbitrariness of ϕ .

To find the compatibility conditions for Eq. (4), We truncate Expression (5) at $j = 3$ as

$$u = \phi^{-a\gamma} \sum_{j=0}^3 q_j^a \phi^j, \quad v = \phi^{-b\beta} \sum_{j=0}^3 r_j^b \phi^j, \quad (11)$$

and substitute Expressions (11) and Constraint (8) into Eq. (4). We make the coefficients of $\phi^{-a\alpha-2-j}$ in Eq. (4a) and $\phi^{a\alpha-3-j}$ in Eq. (4b) at $j = 0, 2$ and 3 to vanish, so that we find that the compatibility condition at $j = 0, 2$ and 3 is satisfied identically with $a = \frac{1}{2}(1 \pm \sqrt{3})$, $b = \frac{1}{2}(1 \mp \sqrt{3})$ and $\gamma = \beta = 1$. The compatibility condition is derived from Constraint (8), as

$$\alpha(t)^2 + 8\lambda(t)v(t) = 0, \quad (12)$$

which is different from that in Ref. [48]. Therefore, under variable-coefficient constraint (12), Eq. (1) is Painlevé integrable.

4 Bilinear forms and soliton solutions for Eq. (1)

Due to Constraint (12), introducing the transformation

$$u = \frac{g}{f}, \quad (13)$$

substituting Eqs. (13) into (1), we derive the bilinear forms for Eq. (1) as

$$[iD_t + \lambda(t)D_x^2](g \cdot f) = 0, \quad (14a)$$

$$\lambda(t)D_x(f \cdot f^*) - \frac{1}{2}i\alpha(t)|g|^2 = 0, \quad (14b)$$

$$\lambda(t)D_x^2(f \cdot f^*) - \frac{1}{2}i\alpha(t)D_x(g \cdot g^*) - \mu(t)|g|^2 = 0, \quad (14c)$$

where g and f are the complex differential functions and the bilinear operators D_t and D_x are defined by [1, 2,61]

$$D_x^p D_t^q (\Phi \cdot \Psi) = \left(\frac{\partial}{\partial x} - \frac{\partial}{\partial x'}\right)^p \left(\frac{\partial}{\partial t} - \frac{\partial}{\partial t'}\right)^q \times \Phi(x, t) \Psi(x', t')|_{t'=t, x'=x}, \quad (15)$$

where $\Phi(x, t)$ is a differentiable function with respect to x and t , $\Psi(x', t')$ is a differentiable function with

respect to the formal variables x' and t' , while p and q are both the positive integers.

Note that the N -soliton solutions for Eq. (1) are marked as u_N , where N is a positive integer. Based on Eqs. (13) and (14), expanding f and g , the N -soliton solutions for Eq. (1) can be expressed as

$$u_N = \frac{g}{f}, \tag{16}$$

with

$$f = 1 + \sum_{n=1}^N \varepsilon^{2n} f_{2n}, \quad g = \sum_{n=1}^N \varepsilon^{2n-1} g_{2n-1}, \tag{17}$$

where n is a positive integer and ε is a formal expansion parameter.

4.1 One-soliton solutions for Eq. (1)

Truncating Eq. (17) at $N = 1$ and setting $\varepsilon = 1$, we solve Eq. (14) and obtain the analytic one-soliton solutions for Eq. (1) as

$$u_1 = \frac{g_1}{1 + f_2} = \frac{m_1}{2\sqrt{m_{12}}} \operatorname{sech} [\operatorname{Re}(\theta_1) + \ln \sqrt{m_{12}}] e^{i\operatorname{Im}(\theta_1)}, \tag{18}$$

with

$$\theta_1 = k_1 x + ik_1^2 \int \lambda(t) dt, \quad g_1 = m_1 e^{\theta_1},$$

$$f_2 = m_{12} e^{\theta_1 + \theta_1^*}, \quad k_1 = i \frac{m_1 m_{12} m_1^* \alpha(t)}{8[\operatorname{Im}(m_{12})]^2 \lambda(t)} + i \frac{\mu(t)}{\alpha(t)},$$

where m_1 and m_{12} are the complex constants, $\operatorname{Im}(\bullet)$ and $\operatorname{Re}(\bullet)$ denote the imaginary and real parts of \bullet , respectively. Particularly, $\operatorname{Im}(m_{12}) \neq 0$.

4.2 Two-soliton solutions for Eq. (1)

Truncating Eq. (17) at $N = 2$ and setting $\varepsilon = 1$, similar to the process in Sect. 4.1, we can derive the analytic two-soliton solutions for Eq. (1) as

$$u_2 = \frac{g_1 + g_3}{1 + f_2 + f_4}, \tag{19}$$

with

$$\theta_j = k_j x + ik_j^2 \int \lambda(t) dt + \delta_j, \quad g_1 = e^{\theta_1} + e^{\theta_2},$$

$$g_3 = m_{123} e^{\theta_1 + \theta_2 + \theta_1^*} + m_{124} e^{\theta_1 + \theta_2 + \theta_2^*},$$

$$f_2 = m_{13} e^{\theta_1 + \theta_1^*} + m_{24} e^{\theta_2 + \theta_2^*} + m_{23} e^{\theta_2 + \theta_1^*} + m_{14} e^{\theta_1 + \theta_2^*},$$

$$m_{s_1, s_2 + 2} = \frac{[ik_{s_1} \alpha(t) + \mu(t)]}{2(k_{s_1} + k_{s_2}^*)^2 \lambda(t)},$$

$$f_4 = m_{1234} e^{\theta_1 + \theta_2 + \theta_1^* + \theta_2^*},$$

$$m_{s_1, s_2, s_3 + 2} = \frac{(k_{s_1} - k_{s_2})^2 [ik_{s_3}^* \alpha(t) + \mu(t)]}{2(k_{s_1} + k_{s_3}^*)^2 (k_{s_2} + k_{s_3}^*)^2 \lambda(t)},$$

$$m_{1234} = \frac{(k_1 - k_2)^2 (k_1^* - k_2^*)^2 [ik_2 \alpha(t) + \mu(t)]}{4(k_1 + k_1^*)^2 (k_2 + k_1^*)^2 (k_1 + k_2^*)^2 (k_2 + k_2^*)^2} \times [ik_1 \alpha(t) + \mu(t)] \lambda(t)^{-2},$$

where δ_j 's ($j = 1, 2$) are the real constants, $s_1 < s_2$ and $s_1, s_2, s_3 = 1, 2$.

4.3 Three-soliton solutions for Eq. (1)

Truncating Eq. (17) at $N = 3$ and setting $\varepsilon = 1$, similar to the process in Sect. 4.2, we can derive the analytic three-soliton solutions for Eq. (1) as

$$u_3 = \frac{g_1 + g_3 + g_5}{1 + f_2 + f_4 + f_6}, \tag{20}$$

with

$$g_1 = e^{\theta_1} + e^{\theta_2} + e^{\theta_3},$$

$$f_6 = m_{123456} e^{\theta_1 + \theta_2 + \theta_3 + \theta_1^* + \theta_2^* + \theta_3^*},$$

$$g_5 = m_{12345} e^{\theta_1 + \theta_2 + \theta_3 + \theta_1^* + \theta_2^*} + m_{12346} e^{\theta_1 + \theta_2 + \theta_3 + \theta_1^* + \theta_3^*} + m_{12356} e^{\theta_1 + \theta_2 + \theta_3 + \theta_2^* + \theta_3^*},$$

$$g_3 = m_{124} e^{\theta_1 + \theta_2 + \theta_1^*} + m_{125} e^{\theta_1 + \theta_2 + \theta_2^*} + m_{126} e^{\theta_1 + \theta_2 + \theta_3^*} + m_{134} e^{\theta_1 + \theta_3 + \theta_1^*} + m_{135} e^{\theta_1 + \theta_3 + \theta_2^*} + m_{234} e^{\theta_2 + \theta_3 + \theta_1^*} + m_{235} e^{\theta_3 + \theta_2 + \theta_2^*} + m_{136} e^{\theta_1 + \theta_3 + \theta_3^*} + m_{236} e^{\theta_2 + \theta_3 + \theta_3^*},$$

$$f_2 = m_{14} e^{\theta_1 + \theta_1^*} + m_{25} e^{\theta_2 + \theta_2^*} + m_{15} e^{\theta_1 + \theta_2^*} + m_{24} e^{\theta_2 + \theta_1^*} + m_{36} e^{\theta_3 + \theta_3^*} + m_{34} e^{\theta_3 + \theta_1^*} + m_{35} e^{\theta_3 + \theta_2^*} + m_{26} e^{\theta_2 + \theta_3^*} + m_{16} e^{\theta_1 + \theta_3^*},$$

$$f_4 = m_{1245} e^{\theta_1 + \theta_2 + \theta_1^* + \theta_2^*} + m_{1346} e^{\theta_1 + \theta_3 + \theta_1^* + \theta_3^*} + m_{2356} e^{\theta_3 + \theta_2 + \theta_3^* + \theta_2^*} + m_{1246} e^{\theta_1 + \theta_2 + \theta_1^* + \theta_3^*} + m_{1256} e^{\theta_1 + \theta_2 + \theta_2^* + \theta_3^*} + m_{1345} e^{\theta_1 + \theta_3 + \theta_1^* + \theta_2^*} + m_{1356} e^{\theta_1 + \theta_3 + \theta_2^* + \theta_3^*} + m_{2345} e^{\theta_3 + \theta_2 + \theta_1^* + \theta_2^*}$$

$$\begin{aligned}
 &+ m_{2346} e^{\theta_3 + \theta_2 + \theta_1^* + \theta_3^*}, \\
 m_{s_1, s_2 + 3} &= \frac{ik_{s_1} \alpha(t) + \mu(t)}{2\lambda(t) (k_{s_1} + k_{s_2}^*)^2}, \\
 m_{s_1, s_2, s_3 + 3} &= \frac{[ik_{s_3}^* \alpha(t) + \mu(t)] (k_{s_1} - k_{s_2})^2}{2\lambda(t) (k_{s_1} + k_{s_3}^*)^2 (k_{s_2} + k_{s_3}^*)^2}, \\
 m_{s_1, s_2, s_3 + 3, s_4 + 3} &= \frac{(k_{s_1} - k_{s_2})^2 (k_{s_3}^* - k_{s_4}^*)^2}{4\lambda(t)^2 (k_{s_1} + k_{s_3}^*)^2 (k_{s_1} + k_{s_3}^*)^2} \\
 &\times \frac{\prod_{j=s_1, s_2} [ik_j \alpha(t) + \mu(t)]}{(k_{s_2} + k_{s_4}^*)^2 (k_{s_2} + k_{s_4}^*)^2}, \\
 m_{1, 2, 3, s_1 + 3, s_2 + 3} &= \frac{(k_1 - k_2)^2 (k_1 - k_3)^2 (k_3 - k_2)^2}{4\lambda(t)^2 (k_j + k_{s_2}^*)^2 (k_j + k_{s_1}^*)^2} \\
 &\times (k_{s_1}^* - k_{s_2}^*)^2 \prod_{j=s_1, s_2} [ik_j \alpha(t) + \mu(t)], \\
 m_{123456} &= \frac{|k_3 - k_2|^4 |k_1 - k_2|^4 |k_3 - k_1|^4}{8\lambda(t)^3 \prod_{j=1}^3 (k_j + k_1^*)^2 (k_j + k_2^*)^2 (k_j + k_3^*)^2} \\
 &\times \prod_{j=1}^3 [ik_j \alpha(t) + \mu(t)],
 \end{aligned}$$

where $\theta_j = k_j x + ik_j^2 \int \lambda(t) dt + \delta_j$, δ_j 's ($j = 1, 2, 3$) are the real constants, $s_1 < s_2, s_3 < s_4$ and $s_1, s_2, s_3, s_4 = 1, 2, 3$.

4.4 N -soliton solutions for Eq. (1)

Substituting Eqs. (17) into (14), we solve Eq. (14). The analytic N -soliton solutions for Eq. (1),

$$u_N = \frac{g}{f}, \tag{21}$$

are obtained under Constraint (12), while g and f in Eq. (21) are transformed to

$$\begin{aligned}
 g &= \sum_{n=1}^N \varepsilon^{2n-1} \left[\sum_{N_\rho, N'_{\eta-N}}^g \Gamma_{N_1, \dots, N_n, N'_1, \dots, N'_{n-1}} \right. \\
 &\times \left. \exp \left(\sum_{\rho=1}^n \theta_{N_\rho} + \sum_{\eta=1}^{n-1} \theta_{N'_{\eta-N}}^* \right) \right], \tag{22a}
 \end{aligned}$$

$$\begin{aligned}
 f &= 1 + \sum_{n=1}^N \varepsilon^{2n} \left[\sum_{N_\rho, N'_{\eta-N}}^f \Gamma_{N_1, \dots, N_n, N'_1, \dots, N'_n} \right. \\
 &\times \left. \exp \left(\sum_{\rho=1}^n \theta_{N_\rho} + \sum_{j=1}^n \theta_{N'_{\eta-N}}^* \right) \right], \tag{22b}
 \end{aligned}$$

with

$$\theta_n = k_n x + \omega_n(t) + \delta_n, \quad \omega_n(t) = ik_n^2 \int \lambda(t) dt,$$

$$\begin{aligned}
 \Gamma_{N_1, \dots, N_n, N'_1, \dots, N'_{n-1}} &= \frac{\prod_{\rho=1}^{n-1} [ik_{N'_\rho}^* \alpha(t) + \mu(t)]}{[2\lambda(t)]^{n-1} \prod_{\substack{1 \leq \rho \leq n, \\ 1 \leq \rho' \leq n-1}} (k_{N_\rho} + k_{N'_{\rho'}}^*)^2} \\
 &\times \prod_{\substack{\rho \neq \eta, \rho' \neq \eta' \\ 1 \leq \rho, \eta \leq n, \\ 1 \leq \rho', \eta' \leq n-1}} \left[(k_{N_\rho} - k_{N_\eta})^2 (k_{N'_{\rho'-N}}^* - k_{N'_{\eta'-N}}^*)^2 \right], \\
 \Gamma_{N_1, \dots, N_n, N'_1, \dots, N'_n} &= \frac{\prod_{\rho=1}^n [ik_{N_\rho} \alpha(t) + \mu(t)]}{[2\lambda(t)]^n \prod_{1 \leq \rho, \rho' \leq n} (k_{N_\rho} + k_{N'_{\rho'}}^*)^2} \\
 &\times \prod_{\substack{\rho \neq \eta, \rho' \neq \eta' \\ 1 \leq \rho, \eta, \rho', \eta' \leq n}} \left[(k_{N_\rho} - k_{N_\eta})^2 (k_{N'_{\rho'-N}}^* - k_{N'_{\eta'-N}}^*)^2 \right],
 \end{aligned}$$

where $\theta_{N_\rho}, \theta_{N'_{\eta-N}} \in \{\theta_n\}_{n=1}^N$, $N_1 < N_n < N'_1 < N'_n$, $\Gamma_{N_1} = 1$, k_n 's are the complex constants, θ_{N_ρ} 's ($\theta_{N'_\eta}$'s) are different with each other and $\sum_{N_\rho, N'_{\eta-N}}^g$ ($\sum_{N_\rho, N'_{\eta-N}}^f$) indicates the sum of all the possibilities of $\sum_{\rho=1}^n \theta_{N_\rho} + \sum_{\eta=1}^{n-1} \theta_{N'_{\eta-N}}^*$ ($\sum_{\rho=1}^n \theta_{N_\rho} + \sum_{\eta=1}^n \theta_{N'_{\eta-N}}^*$) for n . g and f contain $\sum_{n=1}^N C_N^n C_N^{n-1}$ and $\sum_{n=1}^N C_N^n C_N^n + 1$ terms, respectively. When $\varepsilon = 1$, we can obtain the N -soliton solutions for Eq. (1) via Eq. (22).

5 Asymptotic analysis

Without loss of generality, we conduct the asymptotic analysis on the two-soliton solutions and three-soliton solutions, i.e., u_2 and u_3 , for illustrating the solitonic interactions.

For the two-soliton solutions, when $m_{1234} \neq 0$, we have the following:

Table 1 Properties of the solitonic interaction for the two-soliton solutions

| Solitons $S_{2,\zeta}$ ($\zeta = 1, 2$) | Widths $W_{2,\zeta}$ | Amplitudes $A_{2,\zeta}$ | Velocities $V_{2,\zeta}$ | Initial phases $P_{2,\zeta}^\mp$ ($j \neq \zeta$) | Phase shifts $\Delta_{2,\zeta} = P_{2,\zeta}^- - P_{2,\zeta}^+ $ |
|--|--|---|--|--|--|
| $S_{2,\zeta}^-$ | $\frac{1}{ \text{Re}(k_\zeta) }$ | $\frac{ m_\zeta }{2\sqrt{ m_{\zeta,\zeta+2} }}$ | $2\lambda(t)\text{Im}(k_\zeta) - A_\zeta^a$ | $\frac{-1}{\text{Re}(k_\zeta)} \ln \sqrt{m_{\zeta,\zeta+2}}$ | $\frac{2}{\text{Re}(k_\zeta)} \ln \frac{ k_1 - k_2 }{ k_2 + k_1^* }$ |
| $S_{2,\zeta}^+$ | $\frac{1}{ \text{Re}(k_\zeta) }$ | $\frac{ m_\zeta }{2\sqrt{ m_{\zeta,\zeta+2} }}$ | $2\lambda(t)\text{Im}(k_\zeta) - A_\zeta^a$ | $\frac{-1}{\text{Re}(k_\zeta)} \ln \frac{\sqrt{m_{1234}}}{\sqrt{m_{j,j+2}}}$ | |
| Propagation paths | $\Phi_{2,\zeta}^-: \text{Re}(\theta_\zeta) + \ln \sqrt{m_{\zeta,\zeta+2}} = \text{const.}$ | | $\Phi_{2,\zeta}^+: \text{Re}(\theta_\zeta) + \ln \frac{\sqrt{m_{1234}}}{\sqrt{m_{j,j+2}}} = \text{const.}$ | | |

^a $A_\zeta = \frac{1}{2\lambda(t)\text{Re}(k_\zeta)[k_\zeta\alpha(t) - i\mu(t)]} \{k_\zeta [\lambda(t)\alpha(t)' - \alpha(t)\lambda(t)'] - i [\lambda(t)\mu(t)' - \mu(t)\lambda(t)']\}$, where $\bullet' = \partial_t \bullet$

(1) Before the interaction ($t \rightarrow -\infty$):

$$S_{21}^- = \frac{m_1}{2\sqrt{m_{13}}} \text{sech} [\text{Re}(\theta_1) + \ln \sqrt{m_{13}}] e^{i\text{Im}(\theta_1)},$$

$$[\text{Re}(\theta_2) \rightarrow -\infty, \text{Re}(\theta_1) \rightarrow 0], \tag{23a}$$

$$S_{22}^- = \frac{m_2}{2\sqrt{m_{24}}} \text{sech} [\text{Re}(\theta_2) + \ln \sqrt{m_{24}}] e^{i\text{Im}(\theta_2)},$$

$$[\text{Re}(\theta_1) \rightarrow -\infty, \text{Re}(\theta_2) \rightarrow 0], \tag{23b}$$

(2) After the interaction ($t \rightarrow +\infty$):

$$S_{21}^+ = \frac{m_{124}}{2\sqrt{m_{24}}\sqrt{m_{1234}}} \text{sech} \left[\text{Re}(\theta_1) + \ln \frac{\sqrt{m_{1234}}}{\sqrt{m_{24}}} \right] e^{i\text{Im}(\theta_1)},$$

$$[\text{Re}(\theta_2) \rightarrow +\infty, \text{Re}(\theta_1) \rightarrow 0], \tag{24a}$$

$$S_{22}^+ = \frac{m_{123}}{2\sqrt{m_{13}}\sqrt{m_{1234}}} \text{sech} \left[\text{Re}(\theta_2) + \ln \frac{\sqrt{m_{1234}}}{\sqrt{m_{13}}} \right] e^{i\text{Im}(\theta_2)},$$

$$[\text{Re}(\theta_1) \rightarrow +\infty, \text{Re}(\theta_2) \rightarrow 0], \tag{24b}$$

where $S_{2,\zeta}^-$'s (or $S_{2,\zeta}^+$'s) denote the asymptotic expressions for the two solitons $S_{2,\zeta}$'s ($\zeta = 1, 2$) before (or after) the interaction for u_2 , respectively. Based on Eqs. (23) and (24), the relevant properties of each soliton during the interaction for u_2 , including the widths $W_{2,\zeta}$, amplitudes $A_{2,\zeta}$, velocities $V_{2,\zeta}$, initial phases $P_{2,\zeta}^\mp$, phase shifts $\Delta_{2,\zeta}$ and propagation paths $\Phi_{2,\zeta}^\mp$, are listed in Table 1, where the first subscript corresponds to the two-soliton solutions, while the second subscript corresponds to the ζ th soliton within the two-soliton solutions.

For the three-soliton solutions, when $m_{123456} \neq 0$, we have the following:

(3) Before the interaction ($t \rightarrow -\infty$):

$$S_{31}^- = \frac{1}{2\sqrt{m_{14}}} \text{sech} [\text{Re}(\theta_1) + \ln \sqrt{m_{14}}] e^{i\text{Im}(\theta_1)},$$

$$[\text{Re}(\theta_3), \text{Re}(\theta_2) \rightarrow -\infty, \text{Re}(\theta_1) \sim 0], \tag{25a}$$

$$S_{32}^- = \frac{1}{2\sqrt{m_{25}}} \text{sech} [\text{Re}(\theta_2) + \ln \sqrt{m_{25}}] e^{i\text{Im}(\theta_2)},$$

$$[\text{Re}(\theta_3), \text{Re}(\theta_1) \rightarrow -\infty, \text{Re}(\theta_2) \sim 0], \tag{25b}$$

$$S_{33}^- = \frac{1}{2\sqrt{m_{36}}} \text{sech} [\text{Re}(\theta_3) + \ln \sqrt{m_{36}}] e^{i\text{Im}(\theta_3)},$$

$$[\text{Re}(\theta_2), \text{Re}(\theta_1) \rightarrow -\infty, \text{Re}(\theta_3) \sim 0], \tag{25c}$$

(4) After the interaction ($t \rightarrow +\infty$):

$$S_{31}^+ = \frac{e^{i\text{Im}(\theta_1)} m_{12356}}{2\sqrt{m_{2356}}\sqrt{m_{123456}}} \times \text{sech} \left[\text{Re}(\theta_1) + \ln \frac{\sqrt{m_{123456}}}{\sqrt{m_{2356}}} \right],$$

$$[\text{Re}(\theta_3), \text{Re}(\theta_2) \rightarrow +\infty, \text{Re}(\theta_1) \sim 0], \tag{26a}$$

$$S_{32}^+ = \frac{e^{i\text{Im}(\theta_2)} m_{12346}}{2\sqrt{m_{1346}}\sqrt{m_{123456}}} \times \text{sech} \left[\text{Re}(\theta_2) + \ln \frac{\sqrt{m_{123456}}}{\sqrt{m_{1346}}} \right],$$

$$[\text{Re}(\theta_3), \text{Re}(\theta_1) \rightarrow +\infty, \text{Re}(\theta_2) \sim 0], \tag{26b}$$

$$S_{33}^+ = \frac{e^{i\text{Im}(\theta_3)} m_{12345}}{2\sqrt{m_{1245}}\sqrt{m_{123456}}} \times \text{sech} \left[\text{Re}(\theta_3) + \ln \frac{\sqrt{m_{123456}}}{\sqrt{m_{1245}}} \right],$$

$$[\text{Re}(\theta_2), \text{Re}(\theta_1) \rightarrow +\infty, \text{Re}(\theta_3) \sim 0], \tag{26c}$$

where $S_{3,\xi}^-$'s (or $S_{3,\xi}^+$'s) denote the asymptotic expressions for the three solitons $S_{3,\xi}$'s ($\xi = 1, 2, 3$) before (or after) the interaction for u_3 , respectively. Based on Eqs. (25) and (26), the relevant properties for each soliton during the interaction for u_3 , including the widths $W_{3,\xi}$, amplitudes $A_{3,\xi}$, velocities $V_{3,\xi}$, initial phases $P_{3,\xi}^\mp$, phase shifts $\Delta_{3,\xi}$ and propagation paths $\Phi_{3,\xi}^\mp$ are listed in Table 2, where the first subscript corresponds to

Table 2 Properties of the solitonic interaction for the three-soliton solutions

| Solitons | Widths $W_{3,\xi}$ | Amplitudes $A_{3,\xi}$ | Velocities $V_{3,\xi}$ | Initial phases | Phase shifts |
|-----------------------------|--|-------------------------------------|--|---|--|
| $S_{3,\xi} (\xi = 1, 2, 3)$ | | | | $P_{3,\xi}^\mp (j < k) (j \neq k \neq \xi)$ | $\Delta_{3,\xi} = P_{3,\xi}^- - P_{3,\xi}^+ $ |
| $S_{3,\xi}^-$ | $\frac{1}{ \text{Re}(k_\xi) }$ | $\frac{1}{2\sqrt{ m_{\xi,\xi+3} }}$ | $2\lambda(t)\text{Im}(k_\xi) - \Lambda_\xi^a$ | $\frac{-\ln m_{\xi,\xi+3}}{2\text{Re}(k_\xi)}$ | $\frac{2}{\text{Re}(k_\xi)} \ln \frac{ k_\xi - k_j k_\xi - k_k }{ k_\xi^* + k_j k_\xi^* + k_k }$ |
| $S_{3,\xi}^+$ | $\frac{1}{ \text{Re}(k_\xi) }$ | $\frac{1}{2\sqrt{ m_{\xi,\xi+3} }}$ | $2\lambda(t)\text{Im}(k_\xi) - \Lambda_\xi^b$ | $\frac{-\ln \frac{m_{123456}}{m_{j,k,j+3,k+3}}}{2\text{Re}(k_\xi)}$ | |
| Propagation paths | $\Phi_{3,\xi}^-: \text{Re}(\theta_\xi) + \ln \sqrt{ m_{\xi,\xi+3} } = \text{const.}$ | | $\Phi_{3,\xi}^+: \text{Re}(\theta_\xi) + \ln \frac{\sqrt{ m_{123456} }}{\sqrt{ m_{j,k,j+3,k+3} }} = \text{const.}$ | | |

^a $\Lambda_\xi = \frac{1}{2\lambda(t)\text{Re}(k_\xi)[k_\xi\alpha(t) - i\mu(t)]} \{k_\xi [\lambda(t)\alpha(t)' - \alpha(t)\lambda(t)'] - i [\lambda(t)\mu(t)' - \mu(t)\lambda(t)']\}$, where $\bullet' = \partial_t \bullet$

the three-soliton solutions, while the second subscript corresponds to the ξ th soliton within the three-soliton solutions.

Based on Tables 1 and 2, the widths $W_{N,\varrho}$, amplitudes $A_{N,\varrho}$ and velocities $V_{N,\varrho}$ ($N = 2, 3$ and $\varrho = \zeta, \xi$) keep unchanged after the interaction, and then the interaction between (or among) the two (or three) solitons may be elastic or inelastic with the phase shifts $\Delta_{N,\varrho}$'s when $m_{1234} \neq 0$ (or $m_{123456} \neq 0$). $A_{N,\varrho}$, $P_{N,\varrho}^\mp$ and $V_{N,\varrho}$ are related to $\alpha(t)$, $\lambda(t)$ and $\mu(t)$ while the $W_{N,\varrho}$ and $\Delta_{N,\varrho}$ are related to the wave numbers k_ϱ 's but not $\alpha(t)$, $\lambda(t)$ and $\mu(t)$.

When $\Lambda_\varrho = 0$, $\alpha(t) = \rho_1\lambda(t) = \rho_2\mu(t)$, where ρ_1 and ρ_2 are the constants. The $V_{N,\varrho}$ and $\Phi_{N,\varrho}^\mp$ ($N = 2, 3$ and $\varrho = \zeta, \xi$) for each soliton can be reduced as

$$V_{N,\varrho} = 2\lambda(t) \text{Im}(k_\varrho), \tag{27}$$

and

$$\begin{aligned} \Phi_{N,\varrho}^- : & \text{Re}(k_\varrho) \left[x - 2\text{Im}(k_\varrho) \int \lambda(t) dt \right] \\ & + \frac{1}{2} \ln \frac{(1 + ik_\varrho\rho_2)\rho_1}{8\text{Re}(k_\varrho)^2\rho_2} = \text{const.}, \end{aligned} \tag{28a}$$

$$\begin{aligned} \Phi_{N,\varrho}^+ : & \text{Re}(k_\varrho) \left[x - 2\text{Im}(k_\varrho) \int \lambda(t) dt \right] \\ & + \frac{1}{2} \ln \frac{(1 + ik_\varrho\rho_2)\rho_1}{8\text{Re}(k_\varrho)^2\rho_2} \\ & + 2 \ln \prod_{N'}^{1, \dots, \widehat{\varrho}, \dots, N} \frac{|k_\varrho - k_{N'}|}{|k_\varrho + k_{N'}^*|} = \text{const.}, \end{aligned} \tag{28b}$$

where $\widehat{\varrho}$ indicates the ϱ is omitted. Particularly, the $A_{N,\varrho}$ and $P_{N,\varrho}^\mp$ ($N = 2, 3$) are only related to k_ϱ 's, while the velocities are related to $\lambda(t)$ and k_ϱ 's under

$\Lambda_\varrho = 0$. According to Eq. (28), $\Phi_{N,\varrho}^\mp$ for each soliton are related to $\lambda(t)$ and k_ϱ 's.

When $\Lambda_\varrho \neq 0$, the relations among $\alpha(t)$, $\lambda(t)$ and $\mu(t)$ are nonlinear. The $V_{N,\varrho}$ and $\Phi_{N,\varrho}^\mp$ ($N = 2, 3$ and $\varrho = \zeta, \xi$) for each soliton are related to $\alpha(t)$, $\beta(t)$, $\mu(t)$ and k_ϱ and derived from Tables 1 and 2, as

$$\begin{aligned} V_{N,\varrho} = & 2\lambda(t) \text{Im}(k_\varrho) - \frac{k_\varrho [\lambda(t)\alpha(t)' - \alpha(t)\lambda(t)']}{2\lambda(t)\text{Re}(k_\varrho) [k_\varrho\alpha(t) - i\mu(t)]} \\ & + \frac{i [\lambda(t)\mu(t)' - \mu(t)\lambda(t)']}{2\lambda(t)\text{Re}(k_\varrho) [k_\varrho\alpha(t) - i\mu(t)]} \end{aligned} \tag{29}$$

and

$$\begin{aligned} \Phi_{N,\varrho}^- : & \text{Re}(k_\varrho) \left[x - 2\text{Im}(k_\varrho) \int \lambda(t) dt \right] \\ & + \frac{1}{2} \ln \frac{[\mu(t) + ik_\varrho\alpha(t)]}{8\text{Re}(k_\varrho)^2\lambda(t)} = \text{const.}, \end{aligned} \tag{30a}$$

$$\begin{aligned} \Phi_{N,\varrho}^+ : & \text{Re}(k_\varrho) \left[x - 2\text{Im}(k_\varrho) \int \lambda(t) dt \right] \\ & + \frac{1}{2} \ln \frac{[\mu(t) + ik_\varrho\alpha(t)]}{8\text{Re}(k_\varrho)^2\lambda(t)} \\ & + 2 \ln \prod_{N'}^{1, \dots, \widehat{\varrho}, \dots, N} \frac{|k_\varrho - k_{N'}|}{|k_\varrho + k_{N'}^*|} = \text{const.}, \end{aligned} \tag{30b}$$

which are more complex than those in Eqs. (27) and (28) under $\Lambda_\varrho = 0$, i.e., $\alpha(t) = \rho_1\lambda(t) = \rho_2\mu(t)$.

6 Discussion

Due to Constraint (12), $\alpha(t)\lambda(t)\nu(t) \neq 0$. According to Solutions (18), we can obtain the width, amplitude,

Table 3 Properties of the one-soliton solutions

| Soliton | Width | Amplitude | Initial phase | Velocity | Propagation path |
|---------|--------------------------------------|----------------------------------|---|-------------------------------------|---|
| u_1 | $\frac{1}{ \operatorname{Re}(k_1) }$ | $\frac{ m_1 }{2\sqrt{ m_{12} }}$ | $-\frac{1}{\operatorname{Re}(k_1)} \ln \sqrt{m_{12}}$ | $2\lambda(t)\operatorname{Im}(k_1)$ | $\operatorname{Re}(\theta_j) + \ln \sqrt{m_{12}} = \text{const.}$ |

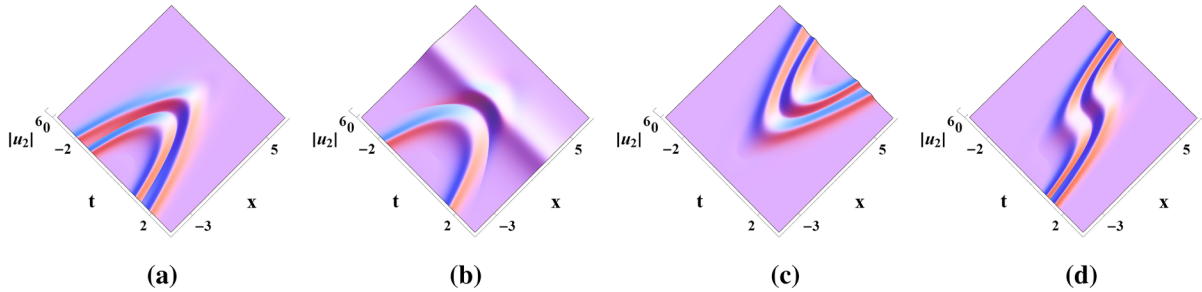


Fig. 1 Interactions between the two solitons for (19) under Constraint (12); **a** $k_1 = 1 - i, k_2 = 1 - 2i$ and $\alpha(t) = \lambda(t) = \mu(t) = t$; **b** the same as **a** except that $k_2 = 1$; **c** the same as **a** except

that $\alpha(t) = \lambda(t) = \mu(t) = -t$; **d** the same as **a** except that $\alpha(t) = \lambda(t) = \mu(t) = t^2$

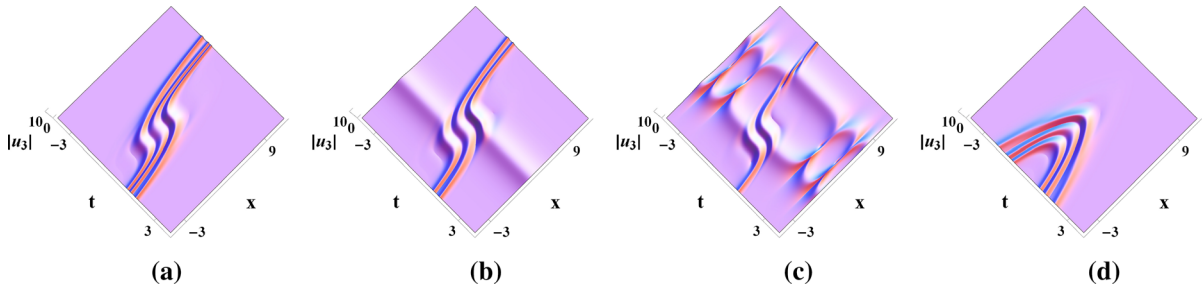


Fig. 2 Interactions among the three solitons for (20) under Constraint (12) with $k_3 = 1 - 2i, \alpha(t) = \lambda(t) = \mu(t) = t^2$; **a** $k_1 = 1 - 3i$ and $k_2 = 1 - i$; **b** $k_1 = 1$ and $k_2 = 1 - i$; **c** $k_1 = 1$ and $k_2 = 1.3$; **d** the same as **a** except that $\alpha(t) = \lambda(t) = \mu(t) = t$

initial phase, velocity and propagation path for the one-soliton solutions, listed in Table 3.

Because the formation of the interaction requires two or more solitons, we will analyze the interactions via Solutions (19) and (20) for Eq. (1). For simplicity, if δ_j 's ($j = 1, 2, 3$) are not mentioned in the figure captions for Solutions (19) and (20), then $\delta_j = 0$. We can see the solitons in Figs. 1–7. We will analyze the interactions under the conditions $\Lambda_\varrho = 0$ and $\Lambda_\varrho \neq 0$, respectively. When $\Lambda_\varrho = 0$, i.e., $\alpha(t) = \rho_1\lambda(t) = \rho_2\mu(t)$, the solitonic interactions are shown in Figs. 1–4.

When $\rho_1 = \rho_2 = 1$ and $\operatorname{Im}(k_\xi)$'s are fixed, according to Eq. (27), parabolic solitons change the propagation directions as $\lambda(t)$ changes from t to $-t$ (or t^2 to $-t^2$), as shown in Fig. 1a, c. According to Eq. (28), the function types of $\lambda(t)$ and the values of $\operatorname{Im}(k_2)$

can both affect the propagation paths, e.g., $\lambda(t) = t$ in Fig. 1a versus $\lambda(t) = t^2$ in Fig. 1d, while $\operatorname{Im}(k_2) = -2$ in Fig. 1a versus $\operatorname{Im}(k_2) = 0$ in Fig. 1b. Particularly, $V_{2,\xi}$ indicates that the corresponding soliton propagates along the t direction, as shown in Fig. 1b.

When $\rho_1 = \rho_2 = 1$, the interactions between/among the bright and parabolic (or hyperbolic) solitons for the two (or three)-soliton solutions are displayed in Fig. 1 (or 2). Figure 2 shows the similar propagation phenomena to Fig. 1, except that when two of $V_{3,\xi}$'s ($\xi = 1, 2, 3$) are equal to zero, the corresponding two bright solitons interact with the hyperbolic soliton, as shown in Fig. 2c, and then the two bright solitons interact with each other and result in the bound solitons.

For the two-soliton solutions, with $\rho_1 = \rho_2 = 1, \lambda(t) = 1$ and $k_2 = -2$, the propagation varies from the interaction between the bright and Kuznetsov–Ma

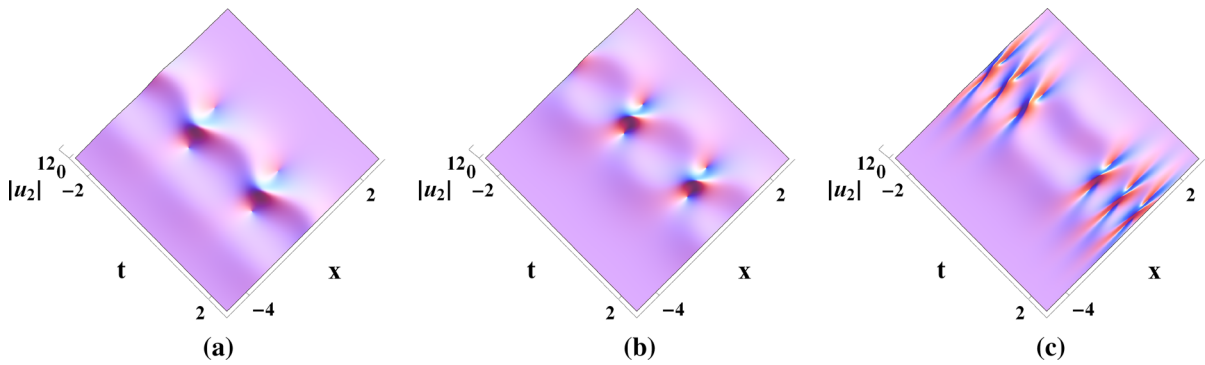


Fig. 3 Interactions between the bright soliton and breathers for (19) under Constraint (12) with $k_2 = -2$; **a** $k_1 = -1$ and $\alpha(t) = \lambda(t) = \mu(t) = 1$ (elastic); **b** $k_1 = 1$ and $\alpha(t) = \lambda(t) = \mu(t) = 1$ (elastic); **c** $k_1 = 1$ and $\alpha(t) = \lambda(t) = \mu(t) = t$ (inelastic)

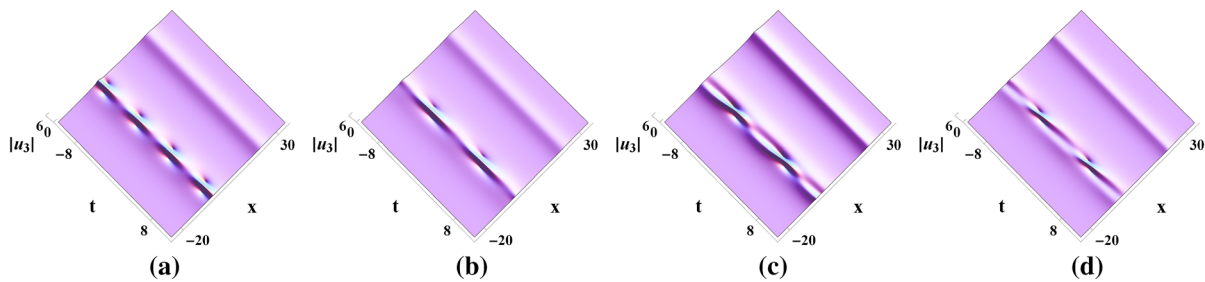


Fig. 4 Interactions among the bright soliton and Kuznetsov–Ma breathers for (20) under Constraint (12) with $k_1 = 1$, $k_2 = 0.3$, $k_3 = 0.4$, $\delta_1 = 5$, $\delta_2 = 1.6$ and $\delta_3 = -3$; **a**

$\alpha(t) = \lambda(t) = \mu(t) = 1$; **b** $\alpha(t) = \mu(t) = 1$ and $\lambda(t) = \frac{2}{3}$; **c** $\alpha(t) = 1$, $\lambda(t) = \frac{2}{3}$ and $\mu(t) = \frac{1}{20}$; **d** $\alpha(t) = 4$, $\lambda(t) = \frac{2}{3}$ and $\mu(t) = \frac{1}{20}$

breathers to the bound solitons, which corresponds to the change of k_1 from -1 to 1 , i.e., Fig. 3a to 3b. Compared with the two solitons in Fig. 3b, when $\lambda(t) = t$, the two solitons interact with each other and result in the bound solitons, as displayed in Fig. 3c.

For the three-soliton solutions, Fig. 4 shows that the interaction between the bright and Kuznetsov–Ma breathers evolves to the interaction between the bright and bound solitons. When $\rho_1 = \rho_2 = 1$, $\delta_1 = 5$, $\delta_2 = 1.6$, $\delta_3 = -3$, $k_1 = 1$, $k_2 = 0.3$ and $k_3 = 0.4$, the bright soliton propagates with the Kuznetsov–Ma breathers in parallel with $\alpha(t) = \lambda(t) = \mu(t) = 1$, as shown in Fig. 4a. Compared with Fig. 4a, Fig. 4b displays that the propagation period changes longer with $\lambda(t) = \frac{2}{3}$. Compared with Fig. 4b, Fig. 4c reveals that the Kuznetsov–Ma breathers evolve to the bound solitons with $\mu(t) = \frac{1}{20}$. Compared with Fig. 4c, Fig. 4d indicates that the amplitudes of the three solitons become lower with $\alpha(t) = 4$.

When $A_\varrho \neq 0$, i.e., the relations among $\alpha(t)$, $\lambda(t)$ and $\mu(t)$ are nonlinear; the solitonic interactions are shown in Figs. 5–7.

With $\alpha(t) = \mu(t) = t$ and $\lambda(t) = t^3$, when $\text{Im}(k_\varrho) = 0$, $V_{N,\varrho} = -\frac{1}{\text{Re}(k_\varrho)} \frac{1}{t}$ ($N = 2, 3$ and $\varrho = \zeta, \xi$) and then the corresponding soliton propagation is not parallel to the t coordinate, as shown in Fig. 5b and 6b (or Figs. 5c, 6c), while $A_{N,\varrho} = \frac{\text{Re}(k_\varrho)}{[1 + \text{Re}(k_\varrho)^2]^{\frac{1}{4}}} |t|$ and then the amplitude is proportional to $|t|$, as shown in Figs. 5 and 6. Amplitudes and velocities of the three solitons change with t during the interaction, implying that the interactions are inelastic.

With the other parameters fixed, $\Phi_{2,\zeta}$'s ($\zeta = 1, 2$) are affected by the integral of $\lambda(t)$ with respect to t and the propagation directions for the two solitons are mutually opposite, as shown in Fig. 7. Propagation path of the two-soliton solutions in Fig. 7c is similar to that in Fig. 7a except that it is compressed by 50% in the

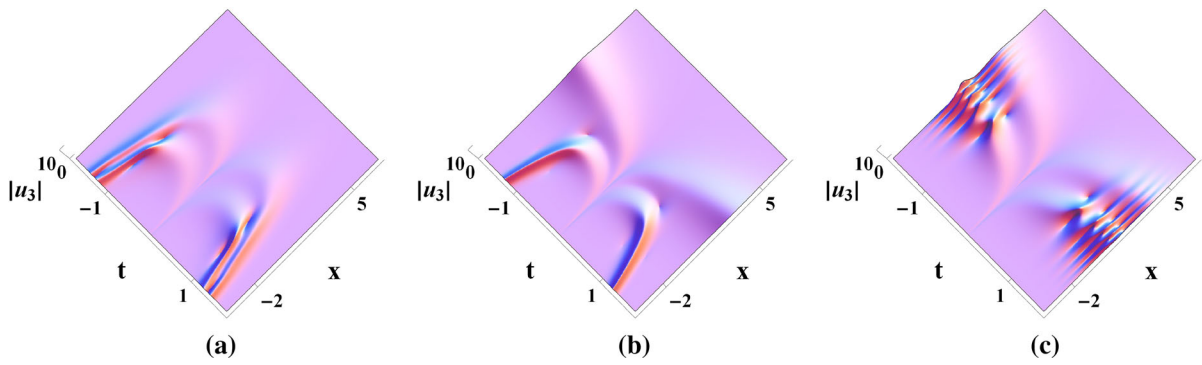


Fig. 5 Inelastic interactions between the solitons for (19) under Constraint (12) with $\alpha(t) = \mu(t) = t$ and $\lambda(t) = t^3$; **a** $k_1 = 1 - i$ and $k_2 = 2 - i$; **b** $k_1 = 1$ and $k_2 = 2 - i$; **c** $k_1 = 1$ and $k_2 = 2$

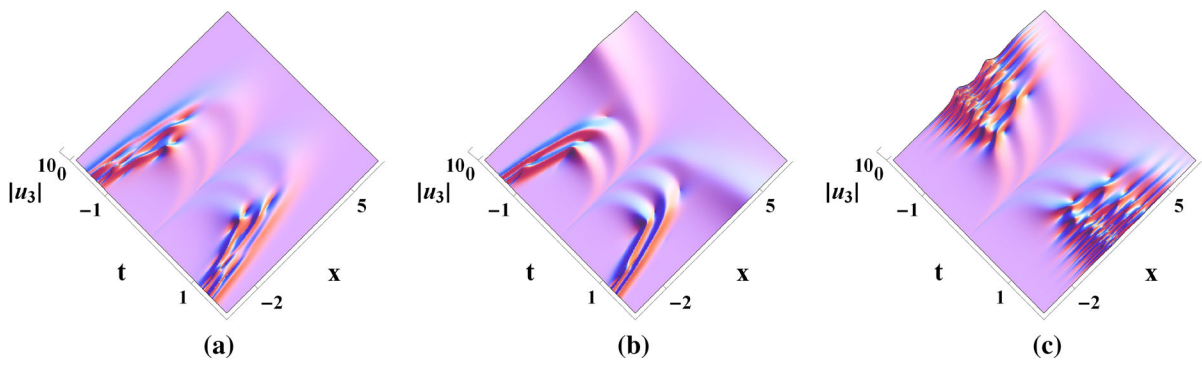


Fig. 6 Inelastic interactions among the solitons for (20) under Constraint (12) with $\alpha(t) = \mu(t) = t$ and $\lambda(t) = t^3$; **a** $k_1 = 1 - i$, $k_2 = 2 - i$ and $k_3 = 3 - i$; **b** $k_1 = 1$, $k_2 = 2 - i$ and $k_3 = 3 - i$; **c** $k_1 = 1$, $k_2 = 2$ and $k_3 = 3$

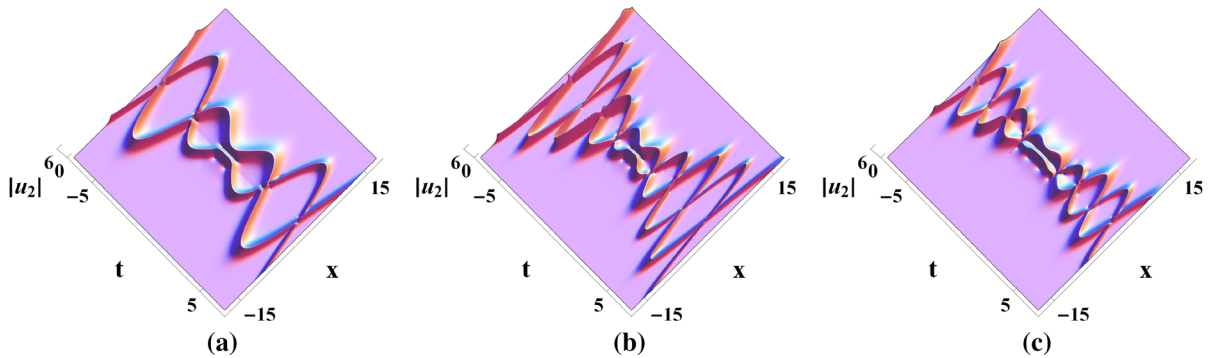


Fig. 7 Inelastic interactions for (19) under Constraint (12) with $\alpha(t) = \mu(t) = \sin(t)$, $k_1 = 1 + i$ and $k_2 = 2 - i$; **a** $\lambda(t) = \sin(t)$; **b** $\lambda(t) = \sin(2t)$; **c** $\lambda(t) = \frac{1}{2}\sin(2t)$

x and t directions, respectively, which is caused by $\lambda(t) = \frac{1}{2}\sin(2t)$.

7 Conclusions

In this paper, attention has been focused on a quintic time-dependent coefficient DNLS equation, i.e.,

Eq. (1), for certain hydrodynamic wave packets or a medium with the negative refractive index. We have found Gauge transformation (2) to obtain the equivalent form of Eq (1), i.e., Eq. (3). With respect to u , the wave envelope for the free water surface displacement or envelope of the electric field, we have obtained variable-coefficient constraint (12), differ-

ent from that in Ref. [48], via the Painlevé analysis, derived N -soliton solutions (21) via bilinear forms (14) and analyzed the solitonic interactions for two-soliton solutions (19) and three-soliton solutions (20) via the asymptotic analysis. Properties for the one-, two- and three-soliton solutions are listed in Tables 1, 2 and 3, respectively.

Based on the asymptotic analysis, classifying the interactions under different conditions, we have revealed two cases of the interactions between (or among) the two (or three) solitons:

Case 1: Relations among the self-steepening coefficient $\alpha(t)$, dispersion coefficient $\lambda(t)$ and cubic nonlinearity $\mu(t)$ are linear. According to Eqs. (27) and (28), velocities $V_{N,\varrho}$'s ($N = 2, 3, \varrho = 1, 2, 3$) and propagation paths $\Phi_{N,\varrho}^{\mp}$'s of the solitons have been both demonstrated to be correlated with $\lambda(t)$. When the propagation paths are $x = \text{const.}$, the corresponding solitons have been observed to propagate along the t direction, as shown in Figs. 1 and 2. With the phase shifts $\Delta_{N,\varrho}$'s changing, we have found that the two solitons in parallel change to the bound solitons, as shown in Fig. 3. It has been observed that the Kuznetsov–Ma breathers change to the bound solitons with $\mu(t) = \frac{1}{20}$ while the propagation period increases as $\lambda(t)$ decreases, as shown in Fig. 4. Interactions are elastic when $\alpha(t)$, $\lambda(t)$ and $\mu(t)$ are constants, as shown in Fig. 4.

Case 2: Relations among $\alpha(t)$, $\lambda(t)$ and $\mu(t)$ are nonlinear. According to Eqs. (29) and (30), amplitude $A_{N,\varrho}$, velocity $V_{N,\varrho}$ and propagation path $\Phi_{N,\varrho}^{\mp}$ of the soliton have been demonstrated to be correlated with $\alpha(t)$, $\lambda(t)$ and $\mu(t)$. Amplitudes $A_{N,\varrho}$'s, velocities $V_{N,\varrho}$'s and propagation paths $\Phi_{N,\varrho}^{\mp}$'s of the two or three solitons change with t during the interactions, implying that the interactions are inelastic, as shown in Figs. 5 and 6. We have found that there is a compression effect on the propagation paths of the two solitons, which is caused by $\lambda(t)$, as shown in Fig. 7.

Acknowledgements We express our sincere thanks to the each member of our discussion group for their valuable suggestions. This work has been supported by the National Natural Science Foundation of China under Grant No. 11772017 and by the

Fundamental Research Funds for the Central Universities under Grant No. 50100002016105010.

Compliance with ethical standards

Conflict of interest The authors declare that they have no conflict of interest.

References

1. Wu, X.Y., Tian, B., Yin, H.M., Du, Z.: Rogue-wave solutions for a discrete Ablowitz–Ladik equation with variable coefficients for an electrical lattice. *Nonlinear Dyn.* **93**, 1635–1645 (2018)
2. Wu, X.Y., Tian, B., Liu, L., Sun, Y.: Rogue waves for a variable-coefficient Kadomtsev–Petviashvili equation in fluid mechanics. *Comput. Math. Appl.* **72**, 215–223 (2018)
3. Feng, L.L., Zhang, T.T.: Breather wave, rogue wave and solitary wave solutions of a coupled nonlinear Schrödinger equation. *Appl. Math. Lett.* **78**, 133–140 (2018)
4. Yuan, Y.Q., Tian, B., Liu, L., Wu, X.Y., Sun, Y.: Solitons for the (2+1)-dimensional Konopelchenko–Dubrovsky equations. *J. Math. Anal. Appl.* **460**, 476–486 (2018)
5. Gao, X.Y.: Looking at a nonlinear inhomogeneous optical fiber through the generalized higher-order variable-coefficient Hirota equation. *Appl. Math. Lett.* **73**, 143–149 (2017)
6. Wang, X.B., Zhang, T.T., Dong, M.J.: Dynamics of the breathers and rogue waves in the higher-order nonlinear Schrödinger equation. *Appl. Math. Lett.* **86**, 298–304 (2018)
7. Gao, X.Y.: Mathematical view with observational/experimental consideration on certain (2+1)-dimensional waves in the cosmic/laboratory dusty plasmas. *Appl. Math. Lett.* **91**, 165–172 (2019)
8. Dong, M.J., Tian, S.F., Yan, X.W., Zou, L.: Solitary waves, homoclinic breather waves and rogue waves of the (3+1)-dimensional Hirota bilinear equation. *Comput. Math. Appl.* **75**, 957–964 (2018)
9. Liu, L., Tian, B., Wu, X.Y., Sun, Y.: Higher-order rogue wave-like solutions for a nonautonomous nonlinear Schrödinger equation with external potentials. *Phys. A* **492**, 524–533 (2018)
10. Sun, Y., Tian, B., Y. Q. Yuan, Du, Z.: Semi-rational solutions for a (2 + 1)-dimensional Davey–Stewartson system on the surface water waves of finite depth. *Nonlinear Dynam.* **94**, 3029–3040 (2018)
11. Wang, X.B., Tian, S.F., Yan, H., Zhang, T.T.: On the solitary waves, breather waves and rogue waves to a generalized (3+1)-dimensional Kadomtsev–Petviashvili equation. *Comput. Math. Appl.* **74**, 556–563 (2017)
12. Zhao, X.H., Tian, B., Xie, X.Y., Wu, X.Y., Sun, Y., Guo, Y.J.: Solitons, Backlund transformation and Lax pair for a (2+1)-dimensional Davey–Stewartson system on surface waves of finite depth. *Wave. Random Complex* **28**, 356–366 (2018)
13. Yan, X.W., Tian, S.F., Dong, M.J., Zhou, L., Zhang, T.T.: Characteristics of solitary wave, homoclinic breather wave and rogue wave solutions in a (2+1)-dimensional generalized breaking soliton equation. *Comput. Math. Appl.* **76**, 179–186 (2018)

14. Yin, H.M., Tian, B., Chai, J., Wu, X.Y.: Stochastic soliton solutions for the $(2+1)$ -dimensional stochastic Broer-Kaup equations in a fluid or plasma. *Appl. Math. Lett.* **82**, 126–131 (2018)
15. Yin, H.M., Tian, B., Chai, J., Liu, L., Sun, Y.: Numerical solutions of a variable-coefficient nonlinear Schrödinger equation for an inhomogeneous optical fiber. *Comput. Math. Appl.* **76**, 1827–1836 (2018)
16. Feng, L.L., Tian, S.F., Wang, X.B., Zhang, T.T.: Rogue waves, homoclinic breather waves and soliton waves for the $(2+1)$ -dimensional B-type Kadomtsev–Petviashvili equation. *Appl. Math. Lett.* **65**, 90–97 (2017)
17. Hu, C.C., Tian, B., Wu, X.Y., Du, Z., Zhao, X.H.: Lump wave-soliton and rogue wave-soliton interactions for a $(3+1)$ -dimensional B-type Kadomtsev–Petviashvili equation in a fluid. *Chin. J. Phys.* **56**, 2395–2403 (2018)
18. Chen, S.S., Tian, B., Liu, L., Yuan, Y.Q., Zhang, C.R.: Conservation laws, binary Darboux transformations and solitons for a higher-order nonlinear Schrödinger system. *Chaos Soliton. Fract.* **118**, 337–346 (2019)
19. Qin, C.Y., Tian, S.F., Wang, X.B., Zhang, T.T., Li, J.: Rogue waves, bright-dark solitons and traveling wave solutions of the $(3+1)$ -dimensional generalized Kadomtsev–Petviashvili equation. *Comput. Math. Appl.* **75**, 4221–4231 (2018)
20. Du, X.X., Tian, B., Wu, X.Y., Yin, H.M., Zhang, C.R.: Lie group analysis, analytic solutions and conservation laws of the $(3+1)$ -dimensional Zakharov–Kuznetsov–Burgers equation in a collisionless magnetized electron–positron-ion plasma. *Eur. Phys. J. Plus* **133**, 378–392 (2018)
21. Peng, W.Q., Tian, S.F., Zhang, T.T.: Analysis on lump, lumpoff and rogue waves with predictability to the $(2+1)$ -dimensional B-type Kadomtsev–Petviashvili equation. *Phys. Lett. A* **382**, 2701–2708 (2018)
22. Lan, Z.Z., Gao, B.: Lax pair, infinitely many conservation laws and solitons for a $(2+1)$ -dimensional Heisenberg ferromagnetic spin chain equation with time-dependent coefficients. *Appl. Math. Lett.* **79**, 6–12 (2018)
23. Lan, Z.Z.: Multi-soliton solutions for a $(2+1)$ -dimensional variable-coefficient nonlinear Schrödinger equation. **86**, 243–248 (2018)
24. Lan, Z.Z., Gao, B., Du, M.J.: Dark solitons behaviors for a $(2+1)$ -dimensional coupled nonlinear Schrödinger system in an optical fiber. *Chaos, Solitons and Fractals* **111**, 169–174 (2018)
25. Hu, C.C., Tian, B., Wu, X.Y., Yuan, Y.Q., Du, Z.: Mixed lump-kink and rogue wave-kink solutions for a $(3+1)$ -dimensional B-type Kadomtsev–Petviashvili equation in fluid mechanics. *Eur. Phys. J. Plus* **133**, 40–48 (2018)
26. Wang, X.B., Tian, S.F., Qin, C.Y., Zhang, T.T.: Characteristics of the solitary waves and rogue waves with interaction phenomena in a generalized $(3+1)$ -dimensional Kadomtsev–Petviashvili equation. *Appl. Math. Lett.* **72**, 58–64 (2017)
27. Tu, J.M., Tian, S.F., Xu, M.J., Ma, P.L., Zhang, T.T.: On periodic wave solutions with asymptotic behaviors to a $(3+1)$ -dimensional generalized B-type Kadomtsev–Petviashvili equation in fluid dynamics. *Comput. Math. Appl.* **72**, 2486–2504 (2016)
28. Guo, D., Tian, S.F., Zhang, T.T., Li, J.: Modulation instability analysis and soliton solutions of an integrable coupled nonlinear Schrödinger system. *Nonlinear Dyn.* **94**, 2749–2761 (2018)
29. Liu, L., Tian, B., Yuan, Y.Q., Du, Z.: Dark-bright solitons and semirational rogue waves for the coupled Sasa–Satsuma equations. *Phys. Rev. E* **97**, 052217 (2018)
30. Du, Z., Tian, B., Chai, H.P., Sun, Y., Zhao, X.H.: Rogue waves for the coupled variable-coefficient fourth-order nonlinear Schrödinger equations in an inhomogeneous optical fiber. *Chaos Soliton. Fract.* **109**, 90–98 (2018)
31. Peng, W.Q., Tian, S.F., Zhang, T.T.: Dynamics of breather waves and higher-order rogue waves in a coupled nonlinear Schrödinger equation. *Europhys. Lett.* **123**, 50005 (2018)
32. Zhang, C.R., Tian, B., Liu, L., Chai, H.P., Du, Z.: Vector breathers with the negatively coherent coupling in a weakly birefringent fiber. *Wave Motion* **84**, 68–80 (2019)
33. Du, Z., Tian, B., Chai, H.P., Yuan, Y.Q.: Vector multi-rogue waves for the three-coupled fourth-order nonlinear Schrödinger equations in an alpha helical protein. *Commun. Nonlinear Sci. Numer. Simul.* **67**, 49–59 (2019)
34. Tian, S.F.: The mixed coupled nonlinear Schrödinger equation on the half-line via the Fokas method. *Proc. R. Soc. A* **472**, 20160588 (2016)
35. Yuan, Y.Q., Tian, B., Chai, H.P., Wu, X.Y., Du, Z.: Vector semirational rogue waves for a coupled nonlinear Schrödinger system in a birefringent fiber. *Appl. Math. Lett.* **87**, 50–56 (2019)
36. Tian, S.F.: Initial-boundary value problems for the general coupled nonlinear Schrödinger equations on the interval via the Fokas method. *J. Differ. Equ.* **262**, 506–558 (2017)
37. Zhang, C.R., Tian, B., Wu, X.Y., Yuan, Y.Q., Du, X.X.: Rogue waves and solitons of the coherently coupled nonlinear Schrödinger equations with the positive coherent coupling. *Phys. Scr.* **90**, 095202 (2018)
38. Tian, S.F., Zhang, T.T.: Long-time asymptotic behavior for the Gerdjikov–Ivanov type of derivative nonlinear Schrödinger equation with time-periodic boundary condition. *Proc. Am. Math. Soc.* **146**, 1713–1729 (2018)
39. Grecu, D., Grecu, A.T., Visinescu, A.: Madelung fluid description of a coupled system of derivative NLS equations. *Rom. J. Phys.* **57**, 180–191 (2012)
40. Xu, T., Chen, Y.: Mixed interactions of localized waves in the three-component coupled derivative nonlinear Schrödinger equations. *Nonlinear Dyn.* **92**, 2133–2142 (2018)
41. Yu, W., Ekici, M., Mirzazadeh, M., Zhou, Q., Liu, W.J.: Periodic oscillations of dark solitons in nonlinear optics. *Nonlinear Dyn.* **165**, 341–344 (2018)
42. Li, M., Tian, B., Liu, W.J., Zhang, H.Q., Wang, P.: Dark and antidark solitons in the modified nonlinear Schrödinger equation accounting for the self-steepening effect. *Phys. Rev. E* **81**, 046606 (2010)
43. Moses, J., Malomed, B.A., Wise, F.W.: Self-steepening of ultrashort optical pulses without self-phase-modulation. *Phys. Rev. A* **76**, 021802 (2007)
44. Chen, H.H., Lee, Y.C., Liu, C.S.: Integrability of nonlinear Hamiltonian systems by inverse scattering method. *Phys. Scr.* **20**, 490–492 (1979)
45. Zhang, Y.H., Guo, L.J., He, J.S., Zhou, Z.X.: Darboux transformation of the second-type derivative nonlinear Schrödinger equation. *Lett. Math. Phys.* **105**, 853–891 (2015)
46. Triki, H., Alqahtani, R.T., Zhou, Q., Biswas, A.: New envelope solitons for Gerdjikov–Ivanov model in nonlinear fiber optics. *Superlattices Microstruct.* **111**, 326–334 (2017)

47. Lü, X., Ma, W.X., Yu, J., Lin, F.H., Khalique, C.M.: Envelope bright- and dark-soliton solutions for the Gerdjikov-Ivanov model. *Nonlinear Dyn.* **82**, 1211–1220 (2015)
48. Rogers, C., Chow, K.W.: Localized pulses for the quintic derivative nonlinear Schrödinger equation on a continuous-wave background. *Phys. Rev. E* **86**, 037601 (2012)
49. Chow, K.W., Yip, L.P., Grimshaw, R.: Novel solitary pulses for a variable-coefficient derivative nonlinear Schrödinger equation. *J. Phys. Soc. Jpn.* **76**, 074004 (2007)
50. Grimshaw, R.H.J., Annenkov, S.Y.: Water wave packets over variable depth: water wave packets over variable depth. *Stud. Appl. Math.* **126**, 409–427 (2011)
51. Triki, H., Wazwaz, A.M.: A new trial equation method for finding exact chirped soliton solutions of the quintic derivative nonlinear Schrödinger equation with variable coefficients. *Wave Random Complex* **27**, 153–162 (2017)
52. Musette, M.: *Painlevé Analysis for Nonlinear Partial Differential Equations*. Springer, Berlin (1998)
53. Schmitz, R.: The WTC and ARS Painlevé tests. *Appl. Math. Lett.* **10**, 5–9 (1997)
54. Ding, C.Y., Zhao, D., Luo, H.G.: Painlevé integrability of two-component nonautonomous nonlinear Schrödinger equations. *J. Phys. A.* **45**, 115203 (2012)
55. Ablowitz, M.J., Segur, H.: Exact linearization of a Painlevé transcendent. *Phys. Rev. Lett.* **38**, 1103–1106 (1977)
56. Guo, R., Hao, H.Q.: Breathers and multi-soliton solutions for the higher-order generalized nonlinear Schrödinger equation. *Commun. Nonlinear Sci. Numer. Simul.* **18**, 2426–2435 (2013)
57. Yu, X., Gao, Y.T., Sun, Z.Y., Meng, X.H., Liu, Y., Feng, Q., Wang, M.Z.: N-soliton solutions for the (2+1)-dimensional Hirota–Maccari equation in fluids, plasmas and optical fibers. *J. Math. Anal. Appl.* **378**, 519–527 (2011)
58. Yajima, T.: Derivative nonlinear Schrödinger type equations with multiple components and their solutions. *J. Phys. Soc. Jpn.* **64**, 1901–1909 (1995)
59. Pashaev, O.K., Lee, J.H.: Relativistic DNLS and Kaup–Newell hierarchy. *Symmetry Integr. Geom.* **13**, 058 (2017)
60. Kaup, D.J., Newell, A.C.: An exact solution for a derivative nonlinear Schrödinger equation. *J. Math. Phys.* **19**, 798–801 (1978)
61. Hirota, R., Nagai, A., Nimmo, J.J.C., Gilson, C.: *The Direct Method in Soliton Theory*. Cambridge University Press, Cambridge (2004)

Publisher's Note Springer Nature remains neutral with regard to jurisdictional claims in published maps and institutional affiliations.